# Reactivity of Cp*Mo(NO)(=CHCMe$_3$) with Olefins and Dienes: C−H Activation Reactions of Molybdenacyclobutanes

Peter M. Graham, Miriam S. A. Buschhaus, Craig B. Pamplin, and Peter Legzdins*

*Department of Chemistry, The University of British Columbia, Vancouver, British Columbia, Canada V6T 1Z1*

*Received February 20, 2008*

Reactions of a variety of cyclic and acyclic olefins with the title alkylidene complex (formed spontaneously by loss of neopentane from Cp*Mo(NO)(CH$_2$CMe$_3$)$_2$ under ambient conditions) result in the initial formation of molybdenacyclobutane complexes (Cp* = C$_5$Me$_5$). These molybdenacyclobutane complexes do not react via olefin metathesis or cyclopropanation pathways, but instead via C−H activation. Thus, when cyclopentene is the olefinic substrate, the direct result of C−H activation at the $\beta$-position of the metallacyclobutane affords a thermally stable allyl hydrido complex that can be isolated. Such an allyl hydride intermediate is not isolable for larger cyclic olefins (cyclohexene, cycloheptene, and cyclooctene) or acyclic olefins (allylbenzene and 1-hexene). Instead, those complexes react further, undergoing a second C−H activation at the allylic position to produce $\eta^4$-trans-diene complexes concomitant with the loss of dihydrogen. Upon heating, these $\eta^4$-trans-diene complexes liberate diene, thereby enabling the 14*e* Cp*Mo(NO) metal fragment to catalyze the oligomerization of cyclic olefins and dienes including cyclohexene and 1,4-cyclohexadiene. In the case of the acyclic olefin allylbenzene, the metal fragment catalyzes a dimerization to (*E*)-(4-methylpent-1-ene-1,5-diyl)dibenzene under ambient conditions.

## Introduction

Since their original isolation by Schrock in the 1970s, alkylidene complexes remain the focus of investigation due to their rich chemistry.[1–15] In particular, the combination of an olefin with an alkylidene complex results in several general reaction types dependent on the transition metal and ligand-set combination employed. In most cases, the initial intermediate formed is a metallacyclobutane; however, the possible reaction pathways then diverge to afford olefin metathesis, cyclopropanation, or C−H activation products (Scheme 1). The C−H activation pathway is the least commonly observed pathway for metallacyclobutanes, and observation of the direct C−H activation product, an allyl hydride, is often impossible.[2]

**Scheme 1**

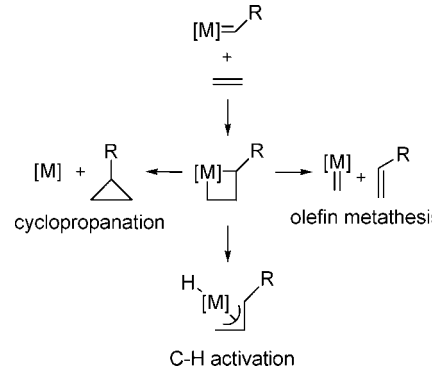


Recently we reported the unusual reactivity of molybdenacyclobutanes formed from the reaction of the molybdenum neopentylidene complex Cp*Mo(NO)(=CHCMe$_3$) (**A**, Scheme 2) with several cyclic olefins.[3] Instead of reacting via olefin metathesis pathways similarly to the well-known molybdenum alkylidene complexes such as the ones developed by Schrock et al.,[4] Cp*Mo(NO)(=CHCMe$_3$) effects intramolecular C−H activations. The present report elucidates this double C−H activation mechanism, examines the scope of reactivity of the molybdenum alkylidene with other olefins and dienes, and explores a further mode of reactivity, namely, the dimerization of olefins catalyzed by the molybdenum $\eta^4$-trans-diene complexes that result from the C−H activation pathway.

* Corresponding author. E-mail: legzdins@chem.ubc.ca.

(1) Schrock, R. R. *J. Am. Chem. Soc.* **1974**, *96*, 6796–6797.
(2) Fryzuk, M. D.; Goa, X.; Rettig, S. J. *J. Am. Chem. Soc.* **1995**, *117*, 3106–3117.
(3) Graham, P. M.; Buschhaus, M. S. A.; Legzdins, P. *J. Am. Chem. Soc.* **2006**, *128*, 9038–9039.
(4) Schrock, R. R.; Czekelius, C. *Adv. Synth. Catal.* **2007**, *349*, 55–77, and references therein.
(5) Wada, K.; Pamplin, C. B.; Legzdins, P.; Patrick, B. O.; Tsyba, I.; Bau, R. *J. Am. Chem. Soc.* **2003**, *125*, 7035–7048.
(6) Legzdins, P.; Pamplin, C. B. Sequential Hydrocarbon C-H Bond Activations by 16-electron Organometallic Complexes of Molybdenum and Tungsten. In *Activation and Functionalization of C-H Bonds*; Goldberg, K. I., Goldman, A. S., Eds.; ACS Symposium Series 885; American Chemical Society: Washington, D.C., 2004; pp 184−197.
(7) Pamplin, C. B.; Legzdins, P. *Acc. Chem. Res.* **2003**, *36*, 223–233.
(8) Basuli, F.; Bailey, B. C.; Huffman, J. C.; Mindiola, D. J. *Organometallics* **2005**, *24*, 3321–3334.
(9) Cheon, J.; Rogers, D. M.; Girolami, G. S. *J. Am. Chem. Soc.* **1997**, *119*, 6804–6813.
(10) Coles, M. P.; Gibson, V. C.; Clegg, W.; Elsegood, M. R. J.; Porrelli, P. A. *J. Chem. Soc., Chem. Commun.* **1996**, *16*, 1963–1964.
(11) van der Heijden, H.; Hessen, B. *J. Chem. Soc., Chem. Commun.* **1995**, *2*, 145–6.
(12) *Handbook of Metathesis*; Grubbs, R. H., Ed.; Wiley-VCH: Weinheim, 2003; Vols. *1*−3: Catalyst Development (Vol. 1); Applications in Organic Synthesis (Vol. 2); Applications in Polymer Synthesis (Vol. 3), and references therein.
(13) Grubbs, R. H. *Tetrahedron* **2004**, *60*, 7117–7140, and references therein.
(14) Schrock, R. R. *Chem. Rev* **2002**, *102*, 145–179, and references therein.
(15) Astruc, D. *New J. Chem.* **2005**, *29*, 42–56, and references therein.

10.1021/om800157s CCC: $40.75 
Publication on Web 05/13/2008

**Scheme 2**

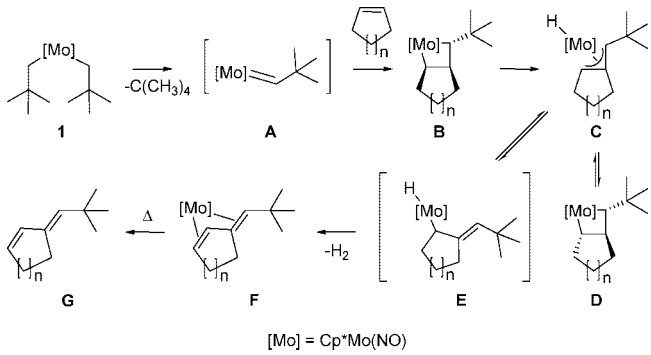


**Scheme 3**

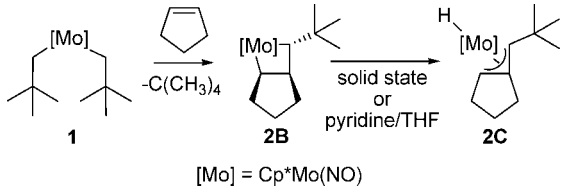


## Results and Discussion

**Cyclic Olefins.** The combination of Cp*Mo(NO)($CH_2CMe_3$)$_2$ (**1**) and cyclic olefins produces a variety of products depending on the substrate used. Varying the cyclic olefin ring size allows the isolation of species representative of several steps (B, C, D, F, and G) along the double C−H activation pathway described in Scheme 2. In no case were products attributable to olefin metathesis or cyclopropanation observed. The alkylidene species **A** has been trapped with pyridine in a previous study.[5]

**Cyclopentene.** An example of the cis metallacycle **B** is synthesized by dissolving **1** in cyclopentene at 20 °C for 18 h, which results in the exclusive formation of orange **2B** (Scheme 3). The $^1$H NMR spectrum of **2B** in $C_6D_6$ includes a characteristic upfield resonance (−0.05 ppm) assigned to the proton in the $\beta$-position of the metallacycle, as well as a downfield resonance (7.94 ppm) attributed to the cyclopentane proton α to the metal. The solid-state molecular structure of **2B** has also been confirmed by a single-crystal X-ray diffraction analysis (Figure 1). The arrangement of C1, C2, C6, and Mo is nearly planar, as evidenced by the C2−C1−C6-Mo1 torsion angle of 0.34(14)°. The protons H1 and H2 are positioned cis, on the same side relative to the ring and away from the Cp* ligand. While the Mo1−C1 distance is within the range for a Mo−C bond, a metal interaction is not depicted formally, as it would result in a five-coordinate carbon.

The isolation of a thermally stable allyl hydride complex **C** (Scheme 2), the result of C−H activation of the $\beta$-hydrogen of the molybdenacyclobutane complex **B**, is also possible. While complex **C** could also be formed via activation at one of the α-positions to give a metallacyclobutene hydride complex that subsequently rearranges to **C** via a 1,2-H shift, no evidence for this path is observed. Rather, **C** appears to form directly from **B**. Specifically, **2C** forms from the parent metallacyclobutane complex **2B** slowly in the solid state at room temperature (Scheme 3). A polar solvent such as THF allows this isomerization to proceed in solution, and the addition of pyridine further accelerates this reaction. The isomerization proceeds very slowly in nonpolar solvents such as $C_6D_6$, with only trace **2C** being observed by $^1$H NMR spectroscopy after 30 days in $C_6D_6$ solution. While no signals attributable to intermediates are

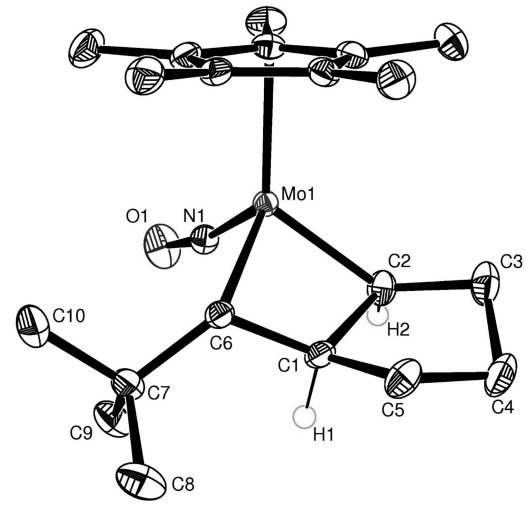


**Figure 1.** Solid-state molecular structure of **2B** with 50% probability thermal ellipsoids shown. Selected interatomic distances (Å) and angles (deg): Mo(1)−C(2) = 2.0599(19), Mo(1)−C(1) = 2.3394(19), Mo(1)−C(6) = 2.1050(18), C(1)−C(2) = 1.693(3), C(1)−C(6) = 1.561(2), Mo(1)−C(2)−C(1) = 76.43(9), Mo(1)−C(6)−C(1) = 77.74(10), C(6)−C(1)−C(2) = 120.42(15), C(2)−Mo(1)−C(6) = 85.41(7), Mo(1)−C(2)−C(3) = 129.43(15), C(6)−C(1)−C(5) = 113.72(16), C(2)−C(1)−C(6)−Mo(1) = 0.34(14).

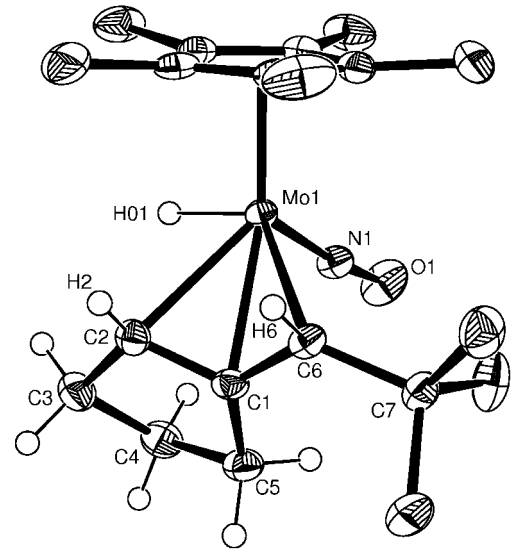


**Figure 2.** Solid-state molecular structure of **2C** with 50% probability thermal ellipsoids shown. Selected interatomic distances (Å) and angles (deg): Mo(1)−C(2) = 2.3581(18), Mo(1)−C(1) = 2.3433(17), Mo(1)−C(6) = 2.3272(17), C(1)−C(2) = 1.397(3), C(1)−C(6) = 1.422(2), C(6)−C(1)−C(2) = 121.17(17), Mo(1)−C(2)−C(1)−C(6) = 55.56(15).

observable, the formation of **2C** is easily monitored by noting the singlet attributable to the molybdenum hydride that appears at −2.04 ppm in the $^1$H NMR spectrum. In addition, the nitrosyl-stretching frequency increases from 1559 cm$^{-1}$ for **2B** to 1609 cm$^{-1}$ for **2C**. Single-crystal X-ray diffraction confirms the allyl structure, with Mo−C bond lengths of 2.33 to 2.36 Å, and the Mo1−H01 linkage (Figure 2).

Complex **2C** is unusual in its thermal stability; such allyl hydride species are often invoked as intermediates in the C−H activation of olefins, but they are not usually observable.[2] Indeed, this C−H activation intermediate can be trapped only in the case of cyclopentene. The smaller ring size of the

**Scheme 4**

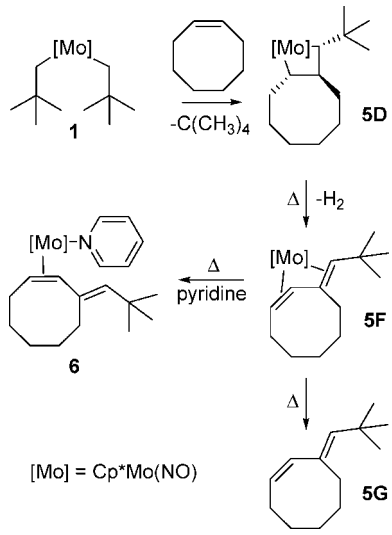


cyclopentene appears key to preventing both potential reaction pathways for **2C**, namely, isomerization to the trans metallacycle (**D**) or a second C−H activation to form the $\eta^4$-trans-diene (**F**, Scheme 2). Formation of **D** is thermodynamically unfavorable due to the ring strain in a trans metallacycle product. Formation of **F** is also precluded, presumably due to the inability of the metal center to access the ring $\beta$-hydrogens required for the second C−H activation in the putative $\eta^1$-allyl intermediate (**E**).

**Cyclooctene.** As shown in Scheme 2, the trans metallacycle **D** differs from the cis metallacycle **B** only in the stereochemical arrangement of the molybdenacyclobutane protons. The reaction of **1** with cyclooctene at 20 °C for 18 h produces metallacycle **5D** exclusively (Scheme 4). The $^{13}$C NMR resonances for the metal-bound carbons of **5D** are similar to those observed for **2B**. Single-crystal X-ray diffraction, however, reveals a metallacycle with a trans orientation of the protons at the bridgehead positions (H1 and H2, Figure 3). The arrangement of C1, C2, C9, and Mo is nearly planar, with a C9−C1−C2−Mo1 torsion angle of 3.42(17)°. Monitoring the reaction of **1** with cyclooctene by $^1$H NMR spectroscopy does not reveal any sign of the cis metallacycle intermediate **B**.

Scheme 2 depicts the allyl hydride **C** as the intermediate between the cis and trans metallacycles **B** and **D**. Examination of the solid-state molecular structures of **2B**, **2C**, and **5D** (Figures 1–3) helps provide insight into the required inversion of stereochemistry around C2. For complex **2B**, H2 points away from the Cp* ligand, but for **5D** H2 points toward the Cp*. The solid-state molecular structure of the isolated allyl hydride complex **2C** clearly exhibits sp$^2$ geometry at C2 of the allyl, which supports the formation of an allyl hydride intermediate during the solution-phase isomerization between the cis and trans metallacycles. The relevant feature of this $\eta^3$-allyl species is the orientation of H2 toward the Cp*, similar to its orientation in **D**. Thus, although the $\beta$-hydrogen (H1) in **B** is the proton that moves from C1 to the metal center, the planarity of the resulting allyl hydride intermediate **C** allows the stereochemical inversion at C2 once H1 is returned to C1 to form **D**. Scheme 5 illustrates this transformation, which features an inversion of stereochemistry at C2 and the intermediacy of a planar $\eta^3$-allyl species **C**.

The isomerization of **2C** to the trans metallacycle form does not occur, and this is not surprising due to the small ring size of cyclopentene (vide supra). For the larger-ring-sized metallacycles the allyl hydride intermediates are not observed,

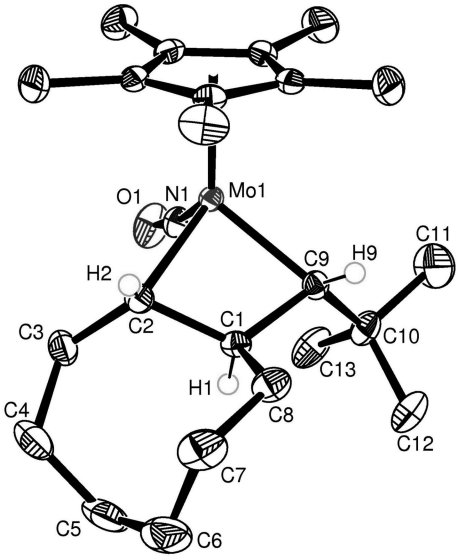


**Figure 3.** Solid-state molecular structure of **5D** with 50% probability thermal ellipsoids shown. Selected interatomic distances (Å) and angles (deg): Mo(1)−C(2) = 2.071(2), Mo(1)−C(9) = 2.070(2), C(1)−C(2) = 1.608(3), C(1)−C(9) = 1.635(3), Mo(1)−C(2)−C(1) = 77.90(11), Mo(1)−C(9)−C(1) = 77.37(11), C(9)−C(1)−C(2) = 119.47(17), C(2)−Mo(1)−C(9) = 85.13(8), Mo(1)−C(2)−C(3) = 126.31(16), C(9)−C(1)−C(8) = 107.25(17), C(9)−C(1)−C(2)−Mo(1) = 3.42(17).

**Scheme 5**

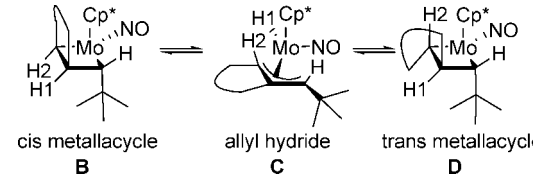


presumably because **D** becomes thermodynamically favored once ring strain is no longer an issue.

Heating of **5D** in cyclohexane at 50 °C for 24 h gives rise to an $\eta^4$-trans-diene species (**5F**) that can be isolated by column chromatography. The $^{13}$C NMR spectrum of **5F** in $C_6D_6$ shows downfield resonances at 121.3, 96.7, 85.2, and 78.0 ppm indicating a metal interaction with four diene carbons (Scheme 4). The dehydrogenation of the cyclooctene-containing ligand can be confirmed by monitoring this transformation by $^1$H NMR spectroscopy in $C_6D_6$, which reveals the growth of a small singlet at 4.56 ppm indicative of the production of $H_2$ over the course of the reaction. The solid-state molecular structure of **5F** has also been confirmed by a single-crystal X-ray diffraction analysis (Figure 4). The structure of **5F** is disordered in the cyclooctenyl ring, specifically carbons C5, C6, and C7. This disorder can be modeled with isotropic carbons in two orientations of 40% and 60% occupancy, with the major orientation being shown in the figure. Unfortunately, this disorder in the structure causes the final *R* value to be high at 6.3%, but it does not compromise the pertinent information about the diene bonding motif. As Scheme 2 shows, this transformation from **D** to **F** is proposed to proceed via back-reaction of **D** to the allyl hydride **C** so that the resulting $\eta^3$-allyl ligand can then isomerize to its $\eta^1$ form (**E**) and allow the second C−H activation event and dehydrogenation to be possible.

**Cycloheptene.** Monitoring the reaction of **1** with cycloheptene in cyclohexane-$d_{12}$ by $^1$H NMR spectroscopy (Figure 5) reveals the stepwise formation of three products (**4B**, then **4D**,

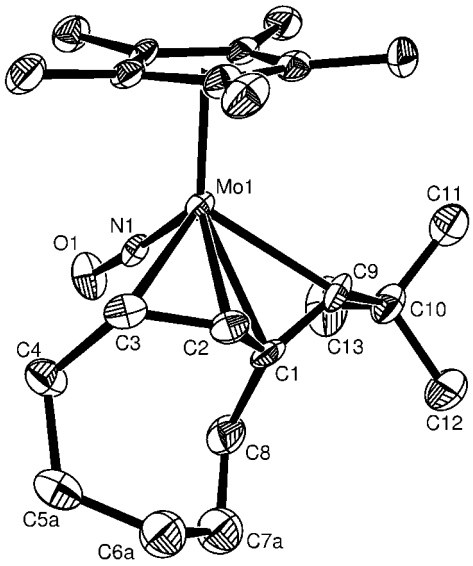


**Figure 4.** Solid-state molecular structure of **5F** with 50% probability thermal ellipsoids shown. Selected interatomic distances (Å) and angles (deg): Mo(1)−C(1) = 2.303(6), Mo(1)−C(2) = 2.182(6), Mo(1)−C(3) = 2.344(7), Mo(1)−C(9) = 2.362(6), C(1)−C(2) = 1.429(9), C(2)−C(3) = 1.426(9), C(1)−C(9) = 1.414(10), C(1)−C(2)−C(3) = 123.4(6), C(2)−C(1)−C(9) = 114.2(5), C(3)−C(2)−C(1)−C(9) = 124.6(7), C(1)−C(2)−C(3)−C(4) = 43.3(10), C(2)−C(1)−C(9)−C(10) = 177.5(6).

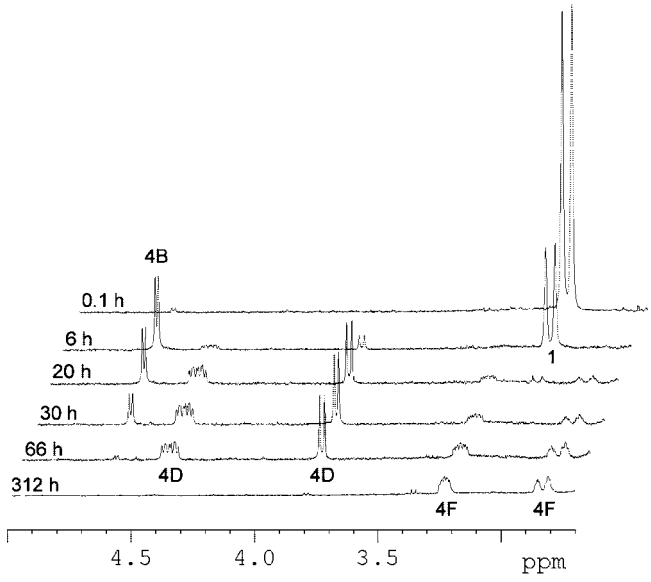


**Figure 5.** Partial $^1$H NMR spectra of reaction of **1** with cycloheptene in cyclohexane-$d_{12}$.

**Scheme 6**

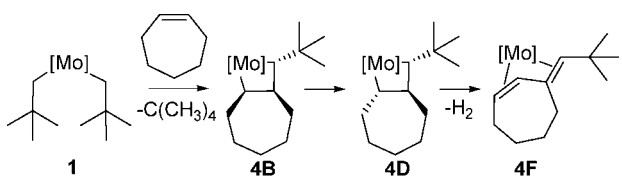


[Mo] = Cp*Mo(NO)

then **4F**) that appear sequentially during the reaction and ultimately result in the exclusive formation of **4F** (Scheme 6). Resonances attributable to **4B** begin to appear within minutes but begin to decrease after 6 h, concomitant with the emergence

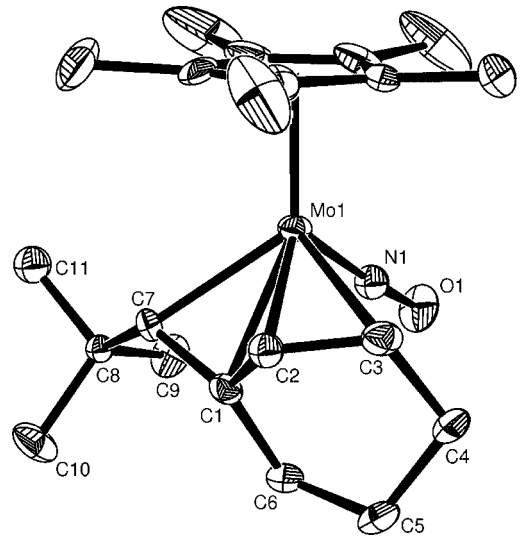


**Figure 6.** Solid-state molecular structure of **3F** with 50% probability thermal ellipsoids shown. Selected interatomic distances (Å) and angles (deg): Mo(1)−C(7) = 2.299(4), Mo(1)−C(1) = 2.233(4), Mo(1)−C(2) = 2.115(9), Mo(1)−C(3) = 2.301(5), C(3)−C(2) = 1.403(8),C(2)−C(1)=1.449(8),C(1)−C(7)=1.427(6),C(3)−C(2)−C(1) = 117.0(6), C(2)−C(1)−C(7) = 114.9(5), C(3)−C(2)−C(1)−C(7) = 126.5(6).

of peaks attributable to **4D**. After nearly a day, the signals for **4F** begin to appear, and after many days they become exclusive. The latter product **4F** can be isolated and purified by column chromatography, and its $^1$H and $^{13}$C NMR spectra indicate a $\eta^4$-trans-diene structure analogous to **5F**. The other two species observed are not amenable to isolation by column chromatography, but **4D** can be crystallized from the reaction mixture after 20 h and spectral data indicate that it is indeed the trans metallacycle. Complex **4B** can be isolated only in combination with **4D**, and its $^1$H and $^{13}$C NMR spectra are most consistent with an assignment as the cis metallacycle **B**. Thus, the reaction with cycloheptene unambiguously connects both molybdenacyclobutane isomers **B** and **D** and further identifies them as precursors to the $\eta^4$-trans-diene complex **F**.

**Cyclohexene.** Not surprisingly, reaction of cyclohexene with **1** leads to the isolation of an $\eta^4$-trans-diene complex **3F** analogous to **4F** and **5F**. Monitoring this reaction by $^1$H NMR spectroscopy shows resonances attributable to at least one intermediate en route to **3F**, likely **3C**. A solid-state molecular structure for **3F** confirms the expected intramolecular geometry and gives a final *R* value of 2.9%, despite mirror-image disorder (Figure 6).

**Reactivity of the $\eta^4$-Diene Complex.** When **5F** is exposed to pyridine at 100 °C for 18 h, the reaction mixture changes from yellow to orange, and a new $\eta^2$-diene complex, **6**, can be isolated by column chromatography (Scheme 4). The $^1$H NMR spectrum of **6** in $C_6D_6$ shows four downfield resonances, three of which are attributable to a metal-bound pyridine ligand. The fourth, a singlet, is assigned to the exocyclic alkene. In addition, single-crystal X-ray diffraction confirms the displacement of the more hindered double bond of the diene and coordination of pyridine into the newly vacated coordination site (Figure 7). The C1−C2 bond length is 1.437(4) Å, the C8−C9 double bond is 1.345(4) Å, and the C1−C8 single bond is 1.484(3) Å. The elongation of the C1−C2 bond, such that the length compares more to the single bond than to the noncoordinated double bond, indicates the expected back-bonding interaction with the metal.

The functionalized cyclooctadiene **5G** can be liberated from the metal by heating **5F** in the presence of an olefin such as

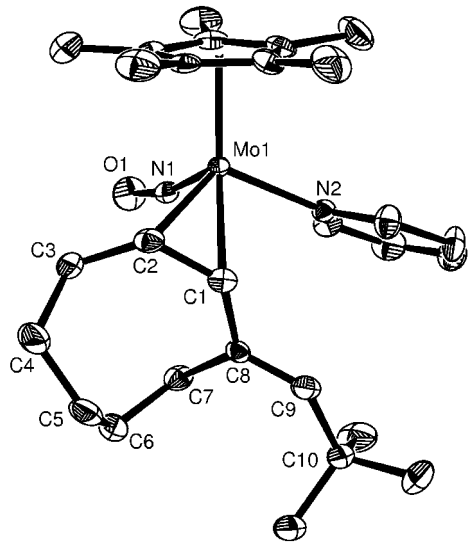


**Figure 7.** Solid-state molecular structure of **6** with 50% probability thermal ellipsoids shown. Selected interatomic distances (Å) and angles (deg): Mo(1)−C(1) = 2.273(3), Mo(1)−C(2) = 2.212(3), Mo(1)−N(2) = 2.192(2), C(1)−C(2) = 1.437(4), C(1)−C(8) = 1.484(3), C(8)−C(9) = 1.345(4), C(2)−C(1)−C(8) = 130.1(2), C(1)−C(8)−C(9) = 117.5(2), C(2)−C(1)−C(8)−C(9) = 161.6(3).

**Scheme 7**

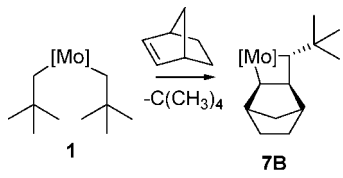


[Mo] = Cp*Mo(NO)

cyclopentene (Scheme 4). In terms of the organic product, the overall reaction is the dehydrogenation and coupling of a cyclic olefin with a neopentylidene group, thereby creating a new diene.

**Norbornene.** In order to confirm that **A** does not react via an olefin-metathesis pathway, **1** has been combined with the strained cyclic olefin norbornene, a traditional ROMP substrate. This reaction produces the cis metallacyclobutane **7B** (Scheme 7), and further reaction is not observed upon heating or addition of pyridine despite **7B** being structurally similar to **2B**.

Indeed the formation of **C** is likely prevented by the added steric constraints of the norbornene bridgehead.

**Summary of Cyclic Olefin Reactivity.** By simply varying the ring size of the cyclic olefin, we have elucidated a general mechanism for the reaction of cyclic olefins with Cp*Mo(NO)(=CHCMe$_3$). A cis metallacycle **B** forms initially upon exposure of **A** to the cyclic olefin. The first C−H activation step then produces an allyl hydride complex **C**. For cyclopentene this allyl hydride complex is isolable, but for larger ring sizes the reaction proceeds further. From **C** the metal-bound hydride can return to the carbon from whence it came along with stereochemical rearrangement to give the trans metallacycle **D**. Alternatively, **C** can isomerize to a proposed $\eta^1$-allyl hydride (**E**), which allows the possibility of a second C−H activation followed by $H_2$ release and formation of the $\eta^4$-trans-diene complex **F**. While the **E** intermediate has not been observed, a species of this type with an open coordination site is required in order for the second C−H activation and dehydrogenation

**Scheme 8**

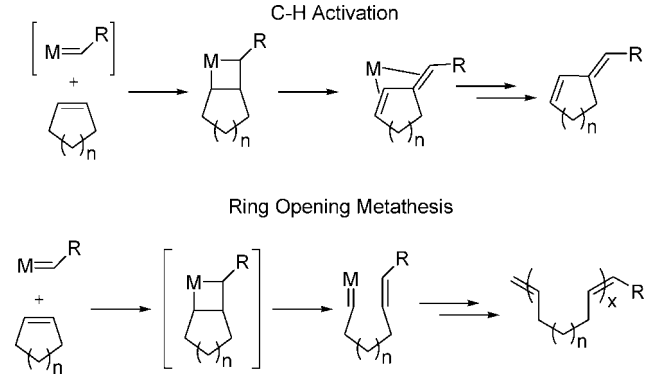


to occur readily. Finally, heating of the $\eta^4$-trans-diene complex **F** liberates the newly constructed diene **G**.

The olefin ring size regulates not only how far along the reaction pathway the complex proceeds but also the relative rate at which it proceeds. For example, cyclohexene forms the $\eta^4$-trans-diene complex (**3F**) in 110 h, while cycloheptene requires over 300 h for exclusive formation of **4F**. Furthermore, cyclooctene does not isomerize to the $\eta^4$-trans-diene form at room temperature and requires heating at 50 °C for 2 days to form **5F**.

This double C−H activation reactivity of cyclic olefins with the alkylidene **A** can be contrasted with the ring-opening metathesis mechanism followed by molybdenum alkylidenes such as the well-established Schrock catalysts (Scheme 8). In contrast to **A**, which is not thermally stable even at room temperature, the Schrock alkylidene complexes are specifically designed to support a stabilized alkylidene and indeed show remarkable thermal stability even at elevated temperatures.[4] The initial production of a molybdenacyclobutane is similar for both complexes, but beyond this point the mechanistic pathways diverge. If ROMP is to be successful, the metallacyclobutane must be fleeting, favoring the facile formation of a new alkylidene to react with further equivalents of olefin and form a polymer chain. By contrast, the C−H activation processes elucidated here form metallacyclobutanes that are often isolable (or at least observable) before they undergo the double C−H activation steps to create $\eta^4$-trans-diene complexes. This double C−H activation process, unprecedented for metallacyclobutane complexes, is perhaps not altogether surprising considering the previously reported C−H activating ability of the Cp*Mo(NO) fragment.[6,7] This ability is often attributed to the electron-rich nature of the fragment, which contrasts with the well-established electron-deficient molybdenum complexes that undergo olefin metathesis.

**Acyclic Olefins.** Reaction of **1** with the acyclic α-olefin 1-hexene gives a single yellow product isolable by column chromatography. Spectroscopic analysis identifies the yellow product as an $\eta^4$-trans-diene complex (**8F**) that is the result of a double C−H activation and dehydrogenation of 1-hexene, analogous to the products observed for cyclic olefins (Scheme 9). A similar product (**9F**) is also formed by 1,7-octadiene. Both products show the characteristic upfield shift of the $^{13}$C NMR resonances attributed metal-coordinated sp$^2$ carbons. With respect to the orientation of R in the $\eta^4$-trans-diene ligand, Scheme 9 indicates **8F** and **9F** are both the *E*,*E* isomers as opposed to *E*,*Z*. This conclusion is supported by the coupling constants ($^3J_{HH}$) observed between H2 and H3, which are 13.7 Hz for **8F** and 13.1 Hz for **9F**. By comparison, the $\eta^4$-*E*,*Z*-trans-dienes synthesized from the cyclic olefins have H2 to H3

**Scheme 9**

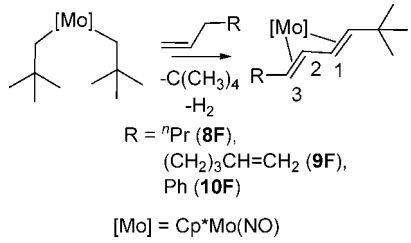


**Scheme 10**

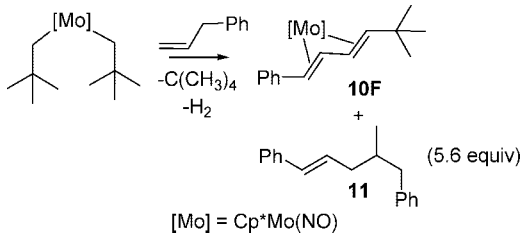


coupling constants of between 6.3 and 9.0 Hz (**3F**, **4F**, **5F**). Additionally, an NOE difference spectroscopy experiment on a sample of **9F** shows an enhanced resonance for H3 when the H1 signal is irradiated (and vice versa) in support of an *E*,*E* rather than *E*,*Z* assignment for the diene. Monitoring these reactions by $^1$H NMR spectroscopy does not detect any intermediates; however a pathway analogous to Scheme 2 involving an initial molybdenacyclobutane **B** that undergoes double C−H activation and loss of $H_2$ seems probable.

**Allylbenzene.** Reaction of **1** with excess allylbenzene in cyclohexane at room temperature for 18 h gives a single organometallic complex as well as a mixture of organic products (Scheme 10). Chromatography of the final reaction mixture on alumina results in the separation of two fractions, a colorless fraction followed by a yellow fraction. The yellow fraction contains the organometallic product **10F**, an $\eta^4$-*E*,*E*-trans-diene complex that resembles **8F** and **9F** and has a H2 to H3 coupling constant of 13.3 Hz. The $^{13}$C NMR resonances attributed to the metal-coordinated carbons exhibit the expected upfield shift. Monitoring by $^1$H NMR spectroscopy does not reveal the presence of any of the presumed intermediates in the double C−H activation mechanism. GC/MS analysis of the product isolated from the colorless fraction indicates an allylbenzene dimer species (**11**) along with traces of the free trans-diene **10G**(Scheme 11). The allylbenzene dimer (**11**) has characteristic olefinic $^1$H NMR resonances: a doublet at 5.72 ppm with a large coupling constant ($^3J_{HH}$ = 15.9 Hz) correlated to a doublet of triplets at 5.50 ppm indicative of an internal double bond with *E* stereochemistry.

The yield of dimer (**11**) can be increased by reacting **1** with 550 equiv of allylbenzene (0.002 mol % Mo) at 100 °C for 18 h to give 83 equiv of allylbenzene dimer. $^1$H NMR spectroscopy of the product mixture reveals that **1** has been fully consumed. In addition, no signals for the $\eta^4$-trans-diene complex **10F** remain. Additional experiments show that heating **10F** or **5F** in the presence of allylbenzene also results in the production of the dimer, thereby confirming that both are precursors to the catalytic species that produces the dimeric product.

Scheme 11 presents the plausible mechanism for production of the observed allylbenzene dimer based on a metallacyclopentane intermediate.[16,17] The trans-diene complex **10F** produces

**Scheme 11**

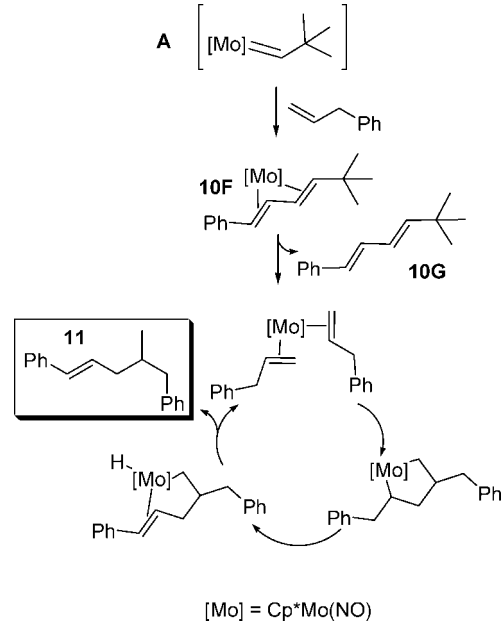


**Scheme 12**

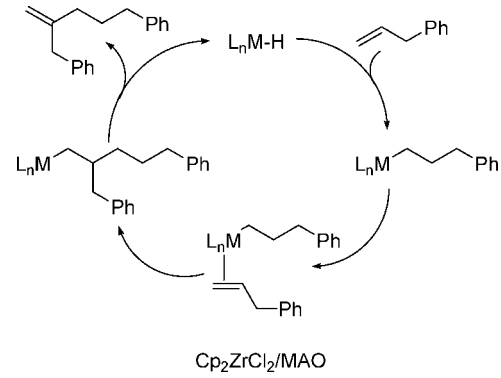


a bis-olefin complex after dissociation of **10G**. The proposed orientation of the olefins minimizes the steric interaction with the Cp* ligand and between the two allylbenzene ligands (phenyl groups facing away from the Cp* and each other). The bis-olefin complex next forms a five-membered metallacycle and subsequently undergoes $\beta$-hydride elimination to give the $\eta^2$-olefin hydride complex. The required $\beta$-hydride elimination is likely favored due to the benzylic nature of the $\beta$-hydrogen. Finally, the complex undergoes reductive elimination to produce the observed dimer and regenerate the putative bis-olefin complex.

The mechanism outlined in Scheme 11 can be contrasted with an established allylbenzene dimerization mechanism invoked by Bergman et al. using a zirconocene/MAO catalyst system (Scheme 12).[18] This mechanism involves the insertion of 2 equiv of allylbenzene into a metal hydride and then metal−carbon bond, followed by a reductive elimination to produce an allylbenzene dimer with an external double bond. As with the above mechanism, the selectivity is controlled sterically with each equivalent of allylbenzene inserting so as to minimize steric interaction with the metal center. However, this olefin-insertion mechanism, as indicated by the disparate product observed, is

(16) McLain, S. J.; Schrock, R. R. *J. Am. Chem. Soc.* **1978**, *100*, 1315–1317.

(17) You, Y.; Wilson, S. R.; Girolami, G. S. *Organometallics* **1994**, *13*, 4655–4657.

(18) Christoffers, J.; Bergman, R. G. *Inorg. Chim. Acta* **1998**, *270*, 20–27.

**Table 1. Dimerization and Trimerization of Olefins and Dienes by 1**[a]

| substrate | product[b] | TON[c] |
|---|---|---|
| cyclohexene | dimer | 7 |
| 1,4-cyclohexadiene | 2:1 dimer:trimer | 12:6 |
| 1,5-cyclooctadiene | dimer | 32 |
| 1,7-octadiene | dimer | ~2 |
| allylbenzene | dimer | 83 |

[a] **1** (5 mg) dissolved in 800 mg of substrate and heated at 100 °C for 18 h. [b] Identified by GC/MS of oligomeric product after elution with pentane through an alumina column. [c] Calculated from mass of oligomeric product isolated by column chromatography.

obviously fundamentally different from the coupling mechanism invoked for **1**.

**Dimerizations.** In light of the ability of **1**and **10F** to dimerize allylbenzene, a series of dimerizations promoted by **1** have been attempted at 100 °C with a range of olefins and dienes. The results are summarized in Table 1. GC/MS analyses of the resulting product mixtures indicate dimerization for all of the substrates except 1,4-cyclohexadiene, which gives a 2:1 mixture of dimers and trimers. Oligomeric products are not observed for conjugated dienes (e.g., 1,3-cyclohexadiene), internal acyclic olefins (e.g., 2-hexene), or cyclic olefins except cyclohexene (cyclopentene, cycloheptene, and cyclooctene). A coupling mechanism analogous to the one depicted in Scheme 11 can be proposed for these olefins and dienes and would produce ring-retaining dimers for cyclic substrates. For example, in the presence of cyclohexene the title complex forms **3F**, which at elevated temperatures loses the $\eta^4$-trans-diene, coordinates 2 equiv of cyclohexene, and dimerizes them via a metallacyclopentane to form a mixture of cyclohexylcyclohexene isomers. Nevertheless, none of the substrates reach the efficiency of allylbenzene, which produces 83 equiv of dimer.

In contrast to cyclohexene, 1,7-octadiene, and allylbenzene, reactions at lower temperatures with 1,4-cyclohexadiene and 1,5-cyclooctadiene do not produce isolable metal complexes. On the whole, **1** does not prove to be an effective dimerization catalyst for any substrate except allybenzene. It thus appears that the benzylic nature of the $\beta$-hydride elimination step in the dimerization mechanism (Scheme 9) is the key factor in enhancing allylbenzene's reactivity over the other olefins and dienes.

**Epilogue.** This work highlights several previously unknown capabilities of the Cp*Mo(NO) fragment. When the fragment supports an alkylidene, the complex is capable of facile C−H activation of olefins and dienes, in contrast to higher-valent molybdenum alkylidene complexes that favor metathesis pathways. However, when the fragment supports two olefins within its coordination sphere, a coupling process occurs that results in the catalytic dimerization (or trimerization) of olefins and unconjugated diene substrates. These distinct processes become connected when the $\eta^4$-trans-diene resulting from C−H activation is labile and can be readily liberated to allow further substrate coordination and dimerization.

The preference for C−H activation of Cp*Mo(NO)(=CHCMe$_3$) instead of olefin metathesis might seem perplexing at first glance, considering many molybdenum alkylidenes are very active olefin metathesis catalysts. However, two observations help explain this preference. First, although both Cp*Mo(NO)(=CHCMe$_3$) and a typical Schrock alkylidene are electronically unsaturated at the metal center, the title complex is low valent, has greater electron density at the molybdenum center, and is thus more capable of activating C−H bonds. Second, the key step in the olefin metathesis pathway involves the metallacyclobutane preferentially forming a new alkylidene complex, and therefore the Schrock complexes are designed to stabilize this alkylidene. Alternatively, Cp*Mo(NO)(=CHCMe$_3$) is quite thermally unstable at room temperature, and thus the formation of a new alkylidene from the metallacyclobutane is quite thermodynamically unfavorable by comparison to both the molybdenacyclobutane **B** and the allyl hydride complex **C**. In summary, the title complex, being electron rich, low valent, and thermally unstable, is fundamentally different from a typical Schrock alkylidene and thus exhibits differing reactivity with olefins.

The reactivity of the related tungsten alkylidene congener is also under investigation in our laboratories. While both the C−H activation and olefin coupling mechanisms invoked here for the molybdenum alkylidene complex appear relevant, isolation of the various intermediate complexes has not been possible. These results will be reported in due course.

The coupling of olefinic substrates in the presence of an alkylidene species by a process other than olefin metathesis is of particular note. Specifically, since the ring-opening-metathesis oligomerization of cyclohexene can be observed only at low temperature,[19] clearly a disparate process is in operation for the title compound. In fact, the puzzling observation of cyclohexene oligomers by early olefin-metathesis investigators using metathesis catalysts generated from $WCl_6$ is more likely the result of a coupling mechanism similar to the one observed here rather than traditional ring-opening metathesis.[20,21] Indeed, it is conceivable that more modern alkylidene complexes designed for olefin metathesis might also exhibit these C−H activation and/or coupling pathways, particularly if they contain sufficient electron density at the metal center. In addition, it is likely that these newly elucidated mechanisms are of relevance to the reaction of already known C−H activating alkylidene complexes of early transition metals with olefins.[8–11] Regardless, these newly elucidated processes further complement the already rich chemistry associated with group six cyclopentadienyl-nitrosyl complexes.[6,7]

## Experimental Section

**General Methods.** All reactions and subsequent manipulations involving organometallic reagents were performed under anaerobic and anhydrous conditions either at a vacuum-nitrogen dual manifold or in an inert-atmosphere drybox. Pentane, benzene-$d_6$, diethyl ether, and tetrahydrofuran (THF) were all dried over sodium benzophenone ketyl and were freshly distilled prior to use. Cyclopentene, cyclohexene, cyclohexane, cycloheptene, cyclooctene, allylbenzene, 1-hexene, and 1,7-octadiene were all purchased from Aldrich and were dried over sodium benzophenone ketyl, distilled, and stored in resealable glass vessels. Cp*Mo(NO)($CH_2CMe_3$)$_2$ (**1**) was prepared according to the published procedure.[5] All other chemicals were purchased from Aldrich and used as received.

All IR samples were prepared as Nujol mulls sandwiched between NaCl plates, and their spectra were recorded on a Thermo Nicolet model 4700 FT-IR spectrometer. NMR spectra were recorded on a Bruker AV400 or AMX 500 instrument, and all chemical shifts and coupling constants are reported in ppm and in Hz, respectively. $^1$H NMR spectra were referenced to the residual protio isotopomer present in $C_6D_6$ (7.16 ppm). $^{13}$C NMR spectra were referenced to $C_6D_6$ (128 ppm). Where necessary, $^1$H−$^1$H

(19) Patton, P. A.; Lillya, C. P.; McCarthy, T. J. *Macromolecules* **1986**, *19*, 1266–1268.
(20) Giezynski, R.; Korda, A. *J. Mol. Catal.* **1980**, *7*, 349.
(21) Moulijn, J. A.; vande Nouland, B. M. *React. Kinet. Catal. Lett.* **1975**, *3*, 405.

**Table 2. X-ray Crystallographic Data for Complexes 2B, 2C, 3F, 5D, 5F, and 6**

| | 2B | 2C | 3F |
|---|---|---|---|
| | Crystal Data | | |
| empirical formula | $C_{20}H_{33}NOMo$ | $C_{20}H_{33}NOMo$ | $C_{21}H_{33}NOMo$ |
| crystal habit, color | prism, orange | plate, yellow | irregular, yellow |
| cryst size (mm) | 0.5 × 0.3 × 0.1 | 0.6 × 0.4 × 0.1 | 0.50 × 0.50 × 0.25 |
| cryst syst | triclinic | monoclinic | monoclinic |
| space group | $P\bar{1}$ | $P2_1/c$ | $P2_1/c$ |
| volume (Å$^3$) | 945.7(2) | 1939.8(1) | 1997.1(4) |
| $a$ (Å) | 8.3346(8) | 13.1444(4) | 8.934(1) |
| $b$ (Å) | 8.4671(8) | 9.1621(3) | 13.776(2) |
| $c$ (Å) | 14.507(1) | 16.7580(5) | 16.5414(8) |
| α (deg) | 84.830(5) | 90 | 90 |
| $\beta$ (deg) | 85.483(5) | 106.020(2) | 101.191(7) |
| $\gamma$ (deg) | 68.227(4) | 90 | 90 |
| $Z$ | 2 | 4 | 4 |
| density (calcd) (Mg/m$^3$) | 1.403 | 1.368 | 1.368 |
| absorp coeff (mm$^{-1}$) | 6.98 | 6.81 | 6.64 |
| $F_{000}$ | 420 | 840 | 864 |
| | Data Collection and Refinement | | |
| measd reflns: total | 6332 | 17 031 | 7285 |
| measd reflns: unique | 3600 | 4608 | 4157 |
| final $R$ indices[a] | R1 = 0.0204, wR2 = 0.0535 | R1 = 0.0244, wR2 = 0.0607 | R1 = 0.0291, wR2 = 0.0713 |
| goodness-of-fit on $F^{2b}$ | 1.068 | 1.031 | 1.069 |
| largest diff peak and hole (e$^-$ Å$^{-3}$) | 0.354 and −0.456 | 0.729 and −0.365 | 0.440 and −0.445 |

| | 5D | 5F | 6 |
|---|---|---|---|
| | Crystal Data | | |
| empirical formula | $C_{23}H_{39}NOMo$ | $C_{23}H_{37}NOMo$ | $C_{28}H_{42}N_2OMo$ |
| cryst habit, color | irregular, red-orange | needle, yellow | block, orange |
| cryst size (mm) | 0.25 × 0.20 × 0.20 | 0.5 × 0.03 × 0.03 | 0.40 × 0.25 × 0.10 |
| cryst syst | monoclinic | orthorhombic | monoclinic |
| space group | $C2/c$ | $Pbca$ | $P2_1/c$ |
| volume (Å$^3$) | 4561.5(8) | 4337.3(10) | 2648.2(6) |
| $a$ (Å) | 19.614(2) | 8.8589(10) | 14.8524(19) |
| $b$ (Å) | 17.114(2) | 17.727(2) | 9.2086(11) |
| $c$ (Å) | 15.519(2) | 27.619(4) | 20.619(3) |
| α (deg) | 90 | 90 | 90 |
| $\beta$ (deg) | 118.880(4) | 90 | 110.106(7) |
| $\gamma$ (deg) | 90 | 90 | 90 |
| $Z$ | 8 | 8 | 4 |
| density (calcd) (Mg/m$^3$) | 1.286 | 1.346 | 1.301 |
| absorp coeff (mm$^{-1}$) | 5.86 | 6.16 | 5.17 |
| $F_{000}$ | 1872 | 1856 | 1096 |
| | Data Collection and Refinement | | |
| measd reflns: total | 7526 | 7680 | 9679 |
| measd reflns: unique | 3966 | 4201 | 5599 |
| final $R$ indices[a] | R1 = 0.0253, wR2 = 0.0591 | R1 = 0.0626, wR2 = 0.1274 | R1 = 0.0338, wR2 = 0.0664 |
| goodness-of-fit on $F^{2b}$ | 1.021 | 1.120 | 0.922 |
| largest diff peak and hole (e$^-$ Å$^{-3}$) | 0.308 and −0.250 | 0.931 and −0.961 | 0.421 and −0.337 |

[a] R1 on $F = \sum(|F_o| - |F_c|)/\sum|F_o|$, ($I > 2\sigma(I)$); wR2 = $[(\sum(F_o^2 - F_c^2)^2)/\sum w(F_o^2)^2]^{1/2}$ (all data); $w = [\sigma^2 F_o^2]^{-1}$. [b] GOF = $[\sum(w(|F_o| - |F_c|)^2)/$degrees of freedom$]^{1/2}$.

COSY, $^1$H−$^{13}$C HMQC, and $^{13}$C APT experiments were carried out to correlate and assign $^1$H and $^{13}$C NMR signals. GC/MS analyses were carried out on an Agilent 6890 Series GC system equipped with a nonpolar, cross-linked 5% diphenyl−95% dimethylpolysiloxane column and an Agilent 5973 Network mass-selective detector. High- and low-resolution mass spectra (EI, 70 eV) were recorded by the staff of the UBC mass spectrometry facility using a Kratos MS-50 spectrometer. Elemental analyses were performed by Mr. Minaz Lakha of the UBC microanalytical facility.

**Complex 2B.** A red solution of Cp*Mo(NO)($CH_2CMe_3$)$_2$ (**1**) (0.079 g, 0.196 mmol) in cyclopentene (10 mL) became orange after 26 h. The final solution was then evaporated to dryness in vacuo, and the residue was recrystallized from diethyl ether/pentane at −30 °C overnight to obtain **2B** as an orange powder (0.039 g, 0.135 mmol, 69%).

Anal. Calcd for $C_{20}H_{33}MoNO$: C, 60.14; H, 3.51; N, 8.33. Found: C, 60.13; H, 3.90; N, 8.06. IR (Nujol): $\nu_{NO}$ 1559 cm$^{-1}$. $^1$H NMR ($C_6D_6$, 400 MHz, 25 °C, $\delta$): 7.94 (1H, dd ($^3J_{HH}$ = 18.7, 8.3), C2*H*), 3.27 (1H, d ($^3J_{HH}$ = 5.2), C6*H*), 2.42 (1H, ddd ($^2J_{HH}$ = 12.4, $^3J_{HH}$ = 8.3, 5.6), C3$H_2$), 1.94 (1H, m (overlapping), C4$H_2$), 1.88 (1H, m (overlapping), C5$H_2$), 1.80 (1H, m (overlapping), C3$H_2$), 1.74 (15H, s, Cp*$CH_3$), 1.70 (1H, m (overlapping), C4$H_2$), 1.15 (9H, s, $^t$Bu$CH_3$), 0.08 (1H, ddd ($^2J_{HH}$ = 23.6, $^3J_{HH}$ = 12.4, 5.2), C5$H_2$), −0.05 (1H, ddd ($^3J_{HH}$ = 18.7, 10.1, 5.2), C1*H*). $^{13}$C{$^1$H} NMR ($C_6D_6$, 100 MHz, 25 °C, $\delta$): 154.2 (C2), 122.7 (C6), 109.7 (Cp* quat), 41.6 ($^t$Bu quat), 39.8 (C4 or C5), 38.4 (C3), 35.9 (C4 or C5), 32.7 ($^t$Bu $CH_3$), 20.4 (C1), 10.7 (Cp*$CH_3$). MS (EI, 120 °C): $m/z$ 401 [M]$^+$.

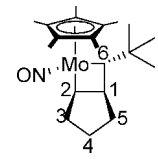


**Complex 2C.** Complex **2B** (0.063 g, 0.158 mmol) was dissolved in THF (4.3 g), to which was added pyridine (0.283 g). The orange solution turned brown over 18 h. The solution was then evaporated

to dryness, and the residue was extracted with pentane (2 mL). The pentane extracts were then loaded onto a column of neutral alumina (3 × 0.5 cm) prepared in pentane. The column was washed with 4:1 pentane/diethyl ether (10 mL). A red-orange band was then eluted using 1:1 pentane/diethyl ether (8 mL) and collected. The red-orange eluate was evaporated to dryness, and the residue was recrystallized from diethyl ether at −30 °C to obtain **2C** as orange crystals (0.022 g, 0.055 mmol, 35%).

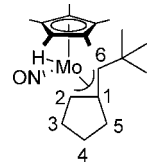


IR (Nujol): $\nu_{NO}$ 1609 cm$^{-1}$. $^1$H NMR ($C_6D_6$, 400 MHz, 25 °C, $\delta$): 2.74 (1H, dd ($^2J_{HH}$ = 13.3, $^3J_{HH}$ = 7.6), C3$H_2$), 2.63 (1H, ddd ($^2J_{HH}$ = 13.3, $^3J_{HH}$ = 10.5, 3.5), C3$H_2$), 2.54 (1H, dd ($^2J_{HH}$ = 14.5, $^3J_{HH}$ = 8.1), C5$H_2$), 2.24 (1H, ddd ($^2J_{HH}$ = 14.5, $^3J_{HH}$ = 11.1, 8.1), C5$H_2$), 1.86 (1H, m, C4$H_2$), 1.76 (1H, m (overlapping), C4$H_2$), 1.73 (15H, s, Cp*$CH_3$), 1.61 (1H, br s, C2$H$), 1.59 (1H, br s, C6$H$), 1.38 (9H, s, $^t$Bu$CH_3$), −2.04 (1H, s, Mo-$H$). $^{13}$C{$^1$H} NMR ($C_6D_6$, 100 MHz, 25 °C, $\delta$): 123.2 (C1), 106.1 (Cp* quat), 81.1 (C2), 80.0 (C6), 36.4 ($^t$Bu quat), 35.4 (C3), 33.8 ($^t$BuCH$_3$), 33.2 (C5), 24.2 (C4), 11.7 (Cp*CH$_3$). HRMS-EI *m*/*z*: [M]$^+$ calcd for $^{98}$MoC$_{20}$H$_{33}$NO 401.16162; found 401.16080.

**Complex 3F.** A red solution of **1** (0.047 g, 0.116 mmol) in cyclohexene (6.64 g) became brown after 110 h. The solution was then evaporated to dryness in vacuo, and the residue was extracted with pentane (2 × 2 mL). The pentane extracts were then loaded onto the top of a column of neutral alumina (2.5 × 0.5 cm) prepared in pentane. The column was washed with pentane (15 mL). A yellow band was eluted with 9:1 pentane/diethyl ether (15 mL) and collected. The yellow eluate was evaporated to obtain **3C** as a yellow solid (0.018 g, 0.044 mmol, 38%). X-ray quality crystals of **3F** could be obtained by dissolving the compound in diethyl ether and slowly allowing the solvent to evaporate over a period of days at room temperature.

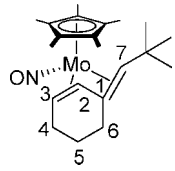


IR (Nujol): $\nu_{NO}$ 1598 cm$^{-1}$. $^1$H NMR ($C_6D_6$, 500 MHz, 25 °C, $\delta$): 3.74 (1H, ddd ($^3J_{HH}$ = 6.7, 6.3, 1.0), C3$H$), 2.52 (1H, dd ($^2J_{HH}$ = 16.5, $^3J_{HH}$ = 4.9), C5$H_2$), 2.30−2.40 (3H, m (overlapping), C4$H_2$ (both), C5$H_2$), 1.70 (1H, s, C7$H$), 1.65 (15H, s, Cp*$CH_3$), 1.54 (2H, m, C6$H_2$), 1.32 (9H, s, $^t$Bu$CH_3$), 1.12 (1H, d ($^3J_{HH}$ = 6.3), C2$H$). $^{13}$C{$^1$H} NMR ($C_6D_6$, 125 MHz, 25 °C, $\delta$): 115.8 (C1), 105.2 (Cp* quat), 94.1 (C7), 85.9 (C2), 76.9 (C3), 34.9 ($^t$Bu quat), 32.9 ($^t$BuCH$_3$), 27.9 (C5), 26.8 (C4), 22.8 (C6), 10.8 (Cp*CH$_3$). MS (EI, 120 °C): *m*/*z* 413 [M]$^+$.

**Complex 4B.** A red solution of **1** (0.036 g, 0.089 mmol) in cycloheptene (0.485 g) and cyclohexane (4.1 g) darkened to red-brown after 6 h. The solution was then evaporated to dryness in vacuo, and the residue was taken into $C_6D_6$ for spectroscopic characterization as a mixture of **4B** and **4D**.

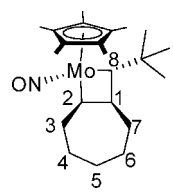


IR (Nujol): $\nu_{NO}$ 1588 cm$^{-1}$. $^1$H NMR ($C_6D_6$, 400 MHz, 25 °C, selected resonances only, $\delta$): 5.66 (1H, dd ($^3J_{HH}$ = 12.7, 9.9), C2$H$), 4.52 (1H, d ($^3J_{HH}$ = 4.2), C8$H$), 2.20 (1H, br d ($^2J_{HH}$ = 12.7), C3$H_2$), 2.00 (1H, m (buried), C7$H_2$), 1.72 (15H, s, Cp*$CH_3$), 1.60 (1H, m (buried), C3$H_2$), 1.22 (9H, s, $^t$Bu$CH_3$), 0.41 (1H, dd ($^2J_{HH}$ = 23.0, $^3J_{HH}$ = 11.0), C7$H_2$), −0.46 (1H, dd ($^3J_{HH}$ = 9.9, 4.2), C1$H$). $^{13}$C{$^1$H} NMR ($C_6D_6$, 100 MHz, 25 °C, selected resonances): 155.5 (C8), 110.2 (C2), 109.6 (Cp* quat), 36.8 (C3), 32.5 ($^t$BuCH$_3$), 31.9 (C7), 10.9 (Cp*CH$_3$).

**Complex 4D.** A red solution of **1** (0.041 g, 0.102 mmol) in cycloheptene (0.521 g) and cyclohexane (8 g) turned brown after 20 h. The final solution was then evaporated to dryness in vacuo. The resulting residue was dissolved in pentane (2 mL), and the solvent was allowed to slowly evaporate over 2 days to produce dark red crystals, which were washed with small aliquots of cold pentane to obtain **4D** (0.011 g, 0.026 mmol, 25%).

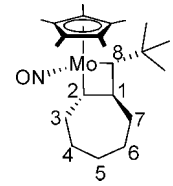


IR (Nujol): $\nu_{NO}$ 1586 cm$^{-1}$. $^1$H NMR ($C_6D_6$, 400 MHz, 25 °C, $\delta$): 4.34 (1H, ddd ($^3J_{HH}$ = 9.2, 5.3, 5.3), C2$H$), 3.71 (1H, d ($^3J_{HH}$ = 6.1), C8$H$), 2.70 (2H, m, C3$H_2$), 2.35 (1H, dddd ($^2J_{HH}$ = 13.3, $^3J_{HH}$ = 6.3, 6.3, 2.4), C7$H_2$), 1.70 (15H, s, Cp*$CH_3$), 1.70 (1H, m (under Cp*), C4$H_2$), 1.60 (2H, m (overlapping), C4$H_2$, C6$H_2$), 1.58 (1H, m (overlapping), C6$H_2$), 1.54 (1H, m (overlapping), C5$H_2$), 1.43 (1H, m (overlapping), C5$H_2$), 1.27 (9H, s, $^t$Bu$CH_3$), 0.35 (1H, ddd ($^2J_{HH}$ = 20.0, $^3J_{HH}$ = 13.3, 6.3), C7$H_2$), −0.28 (1H, dddd ($^3J_{HH}$ = 20.0, 9.2, 6.1, 2.4), C1$H$). $^{13}$C{$^1$H} NMR ($C_6D_6$, 100 MHz, 25 °C, $\delta$): 138.2 (C8), 130.9 (C2), 109.3 (Cp* quat), 41.6 (C3), 32.9 ($^t$BuCH$_3$), 32.7 (C4), 31.5 (C6), 30.0 (C7), 25.2 (C5), 15.2 (C1), 10.7 (Cp*CH$_3$). MS (EI, 120 °C): *m*/*z* 427 [M − 2]$^+$ ($H_2$ is lost upon heating).

**Complex 4F.** A red solution of **1** (0.062 g, 0.154 mmol) in cycloheptene (0.835 g) and cyclohexane (7.2 g) was heated at 50 °C for 20 h. The solution was then evaporated to dryness in vacuo, and the residue was extracted with pentane (2 × 1 mL). The pentane extracts were loaded onto the top of a column of neutral alumina (3 × 1 cm) prepared in pentane. The column was first washed with pentane (3 mL). A yellow band was then eluted with 3:1 pentane/diethyl ether (6 mL) and collected. The yellow eluate was evaporated to dryness in vacuo, and the residue was washed with cold pentane to obtain **4F** as a yellow solid (0.023 g, 0.054 mmol, 35%).

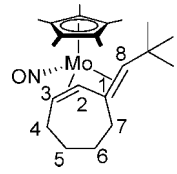


IR (Nujol): $\nu_{NO}$ 1589 cm$^{-1}$. $^1$H NMR ($C_6D_6$, 400 MHz, 25 °C, $\delta$): 3.21 (1H, ddd ($^3J_{HH}$ = 9.0, 4.5, 3.0), C3$H$), 2.90 (1H, d ($^2J_{HH}$ = 17.1), C7$H_2$), 2.72 (1H, m, C4$H_2$), 2.61 (1H, m, C7$H_2$), 2.42 (1H, d ($^2J_{HH}$ = 15.2), C4$H_2$), 1.68 (1H, m (overlapping), C5$H_2$ or C6$H_2$), 1.67 (1H, m (overlapping), C5$H_2$ or C6$H_2$), 1.66 (1H, m (overlapping), C5$H_2$ or C6$H_2$), 1.64 (15H, s, Cp*$CH_3$), 1.63 (1H, m (overlapping), C5$H_2$ or C6$H_2$), 1.40 (1H, s, C8$H$), 1.33 (9H, s, $^t$Bu$CH_3$), 0.21 (1H, d ($^3J_{HH}$ = 9.0), C2$H$). $^{13}$C{$^1$H} NMR ($C_6D_6$, 100 MHz, 25 °C, $\delta$): 123.2 (C1), 105.5 (Cp* quat), 93.6 (C8), 82.2 (C3), 81.1 (C2), 35.5 ($^t$Bu quat), 33.3 (C7), 33.0 ($^t$BuCH$_3$), 33.0 (C4), 26.5 (C5 or C6), 26.4 (C5 or C6), 10.9 (Cp*CH$_3$). MS (EI, 100 °C): *m*/*z* 427 [M]$^+$.

**Complex 5D.** A red solution of **1** (0.063 g, 0.156 mmol) in cyclooctene (0.890 g) was diluted with cyclohexane (10.2 g). The solution darkened to brown after 18 h. The solution was then evaporated to dryness in vacuo, and the residue was extracted with pentane (2 × 1 mL). The pentane extracts were loaded onto the top of a column of neutral alumina (3 × 1 cm) prepared in pentane. The column was washed with pentane (3 mL), and then an orange band was eluted using 5:1 pentane/diethyl ether (6 mL) and collected. The orange eluate was evaporated to dryness in vacuo, the residue was dissolved in minimal pentane, and the resulting solution was stored at −30 °C overnight to induce the deposition of **5D** as red crystals (0.035 g, 0.079 mmol, 51%).

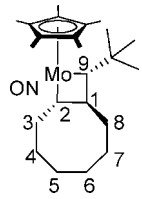


Anal. Calcd for $C_{23}H_{39}MoNO$: C, 62.57; H, 8.90; N, 3.17. Found: C, 62.81; H, 8.60; N, 3.46. IR (Nujol): $\nu_{NO}$ 1586 cm$^{-1}$. $^1$H NMR ($C_6D_6$, 400 MHz, 25 °C, $\delta$): 4.31 (1H, d ($^3J_{HH}$ = 4.4), C9*H*), 4.10 (1H, ddd ($^3J_{HH}$ = 11.7, 4.0, 3.4), C2*H*), 2.79 (1H, ddd ($^2J_{HH}$ = 14.3, $^3J_{HH}$ = 5.8, 3.0), C3$H_2$), 2.45 (1H, m, C3$H_2$), 2.19 (1H, m, C8$H_2$), 1.82 (1H, m (overlapping), C4$H_2$), 1.73 (1H, m (overlapping), C5$H_2$), 1.69 (15H, s, Cp*$CH_3$), 1.64 (1H, m (overlapping), C7$H_2$), 1.51 (1H, m (overlapping), C4$H_2$), 1.50 (1H, m (overlapping), C5$H_2$), 1.48 (1H, m (overlapping), C6$H_2$), 1.46 (1H, m (overlapping), C7$H_2$), 1.36 (1H, m (overlapping), C6$H_2$), 1.28 (9H, s, $^t$Bu$CH_3$), 0.20 (1H, m, C8$H_2$), −0.18 (1H, ddd ($^3J_{HH}$ = 11.7, 7.5, 4.4), C1*H*). $^{13}$C{$^1$H} NMR ($C_6D_6$, 100 MHz, 25 °C, $\delta$): 152.3 (C9), 121.5 (C2), 109.3 (Cp* quat), 44.4 (C3), 44.1 ($^t$Bu quat), 36.1 (C8), 32.9 ($^t$BuCH$_3$), 30.5 (C4), 28.8 (C7), 28.2 (C5 or C6), 28.1 (C5 or C6), 14.9 (C1), 10.7 (Cp*CH$_3$). MS (EI, 100 °C): *m*/*z* 441 [M − 2]$^+$ ($H_2$ is lost upon heating).

**Complex 5F.** An orange solution of **5D** (0.030 g, 0.068 mmol) in cyclohexane (8.0 g) was heated at 50 °C for 48 h. The solution was then evaporated to dryness in vacuo, and the residue was extracted with pentane (2 × 1 mL). The pentane extracts were loaded onto the top of a column of neutral alumina (2 × 1 cm) prepared in pentane. The column was washed with pentane (3 mL), and then a yellow band was eluted using 5:1 pentane/diethyl ether (6 mL) and collected. The yellow eluate was evaporated in vacuo to obtain **5F** as a yellow solid (0.015 g, 0.034 mmol, 50%).

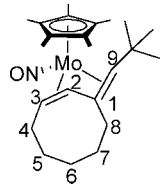


Anal. Calcd for $C_{23}H_{37}MoNO$: C, 62.86; H, 8.49; N, 3.19; Found: C, 62.45; H, 8.59; N, 3.38. IR (Nujol): $\nu_{NO}$ 1595 cm$^{-1}$. $^1$H NMR ($C_6D_6$, 400 MHz, 25 °C, $\delta$): 3.06 (1H, ddd ($^3J_{HH}$ = 16.3, 10.3, 8.0), C3*H*), 2.83 (1H, ddd ($^2J_{HH}$ = 17.1, $^3J_{HH}$ = 5.9, 3.9), C8$H_2$), 2.33 (2H, m (overlapping), C4$H_2$, C6$H_2$), 2.21 (1H, m (overlapping), C8$H_2$), 2.14 (1H, m (overlapping), C4$H_2$), 1.89 (1H, m, C7$H_2$), 1.81 (1H, m (overlapping), C7$H_2$), 1.75 (1H, m (overlapping), C5$H_2$), 1.67 (15H, s, Cp*$CH_3$), 1.66 (1H, s (overlapping), C9*H*), 1.57 (1H, m, C5$H_2$), 1.40 (1H, m, C6$H_2$), 1.30 (9H, s, $^t$Bu$CH_3$), 0.72 (1H, d ($^3J_{HH}$ = 8.0), C2*H*). $^{13}$C{$^1$H} NMR ($C_6D_6$, 100 MHz, 25 °C, $\delta$): 121.3 (C1), 105.6 (Cp* quat), 96.7 (C9), 85.2 (C2), 78.0 (C3), 34.9 ($^t$Bu quat), 33.3 ($^t$BuCH$_3$), 31.8 (C5), 31.3 (C4), 30.1 (C7), 29.0 (C8), 28.0 (C6), 11.3 (Cp*CH$_3$). MS (EI, 100 °C): *m*/*z* 441 [M]$^+$.

**3-Neopentylidene-cyclooctene (5G).** A yellow solution of **5C** (0.021 g, 0.048 mmol) in cyclopentene (2.0 g) was heated at 70 °C for 3 days. The reaction mixture was then evaporated to dryness in vacuo, and the residue was extracted with pentane (2 × 1 mL). The pentane extracts were then loaded onto the top of a column of neutral alumina (2 × 1 cm) prepared in pentane. The column was eluted with pentane, and all the pentane eluates were collected, combined, and evaporated in vacuo to obtain **5G** as a colorless oil (0.04 g, 0.022 mmol, 47%).

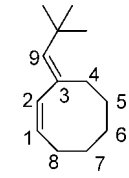


$^1$H NMR ($C_6D_6$, 400 MHz, 25 °C, $\delta$): 6.21 (1H, d ($^3J_{HH}$ = 12.0), C2*H*), 5.57 (1H, s, C9*H*), 5.37 (1H, ddd ($^3J_{HH}$ = 12.0, 8.6, 3.4), C1*H*), 2.64 (2H, t ($^3J_{HH}$ = 6.5), C4$H_2$ (both)), 2.33 (2H, dd ($^3J_{HH}$ = 14.9, 8.6), C8$H_2$ (both)), 1.62 (4H, m, C5$H_2$ (both), C6$H_2$ (both)), 1.48 (2H, m, C7$H_2$ (both)), 1.09 (9H, s, $^t$Bu$CH_3$). $^{13}$C{$^1$H} NMR ($C_6D_6$, 100 MHz, 25 °C, $\delta$): 144.5 (C9), 140.3 (C2), 138.6 (C3), 124.8 (C1), 32.0 ($^t$BuCH$_3$), 28.6 (C7), 28.2 ($^t$Bu quat), 28.1 (C4), 26.5 (C8), 23.2 (C5 or C6), 23.1 (C5 or C6). MS (EI, 100 °C): *m*/*z* 178 [M]$^+$.

**Complex 6.** A yellow solution of **5F** (0.027 g, 0.061 mmol) in pyridine (3.2 g) was heated at 100 °C for 19 h. The reaction mixture was then evaporated to dryness in vacuo, and the residue was extracted with pentane (2 × 1 mL). The pentane extracts were loaded onto the top of a column of neutral alumina (2 × 1 cm) prepared in pentane. The column was washed with 3:1 pentane/diethyl ether (3 mL) to elute any remaining starting material as a yellow band. Next, a red-orange band was eluted using 1:3 pentane/diethyl ether (6 mL) and collected. This eluate was evaporated to dryness in vacuo to give a red residue, which was dissolved in minimal pentane and stored at −30 °C overnight to induce the deposition of **6** as an orange solid (0.023 g, 0.044 mmol, 72%).

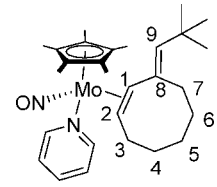


Anal. Calcd for $C_{28}H_{42}MoN_2O$: C, 64.85; H, 8.16; N, 5.40. Found: C, 64.84; H, 8.49; N, 5.80. IR (Nujol): $\nu_{NO}$ 1552 cm$^{-1}$. $^1$H NMR ($C_6D_6$, 400 MHz, 25 °C, $\delta$): 8.07 (2H, br s, ortho pyr), 6.64 (1H, t ($^3J_{HH}$ = 7.5), para pyr), 6.39 (2H, t ($^3J_{HH}$ = 6.4), meta pyr), 4.80 (1H, s, C9*H*), 3.13 (1H, m, C3$H_2$), 2.81 (1H, m, C7$H_2$), 2.57 (1H, m, C4$H_2$), 2.45 (1H, dd ($^3J_{HH}$ = 13.7, 8.6), C7$H_2$), 2.27 (1H, m, C3$H_2$), 1.93 (2H, m (buried), C6$H_2$ (both)), 1.90 (1H, buried, C1*H*), 1.87 (1H, buried, C2*H*), 1.75 (1H, m, C4$H_2$), 1.64 (1H, m, C5$H_2$), 1.53 (15H, s, Cp*$CH_3$), 1.37 (1H, m, C5$H_2$), 0.95 (9H, s, $^t$Bu$CH_3$). $^{13}$C{$^1$H} NMR ($C_6D_6$, 100 MHz, 25 °C, $\delta$): 154.6 (ortho py), 145.1 (C8 (observed by HMBC)), 135.0 (para py), 129.3 (C9), 124.6 (meta py), 105.4 (Cp* quat), 77.1 (C1), 61.9 (C2), 34.7 (C6), 33.1 ($^t$BuCH$_3$), 32.8 (C5), 32.2 (C3), 28.0 ($^t$Bu quat), 26.2 (C7), 23.1 (C4), 9.7 (Cp*CH$_3$). MS (EI, 120 °C): *m*/*z* 520 [M]$^+$.

**Complex 7B. 1** (0.033 g, 0.0820 mmol) was dissolved in cyclohexane (5.5 g) to which was added norbornene (0.110 g). The resulting pink solution darkened to a brown color over 18 h. The solution was then evaporated to dryness, and the residue was extracted with pentane (2 mL). The pentane extracts were loaded onto a column of neutral alumina (3 × 0.5 cm) prepared in pentane. The column was washed with 4:1 pentane/diethyl ether (8 mL). A yellow fraction was then eluted and collected using 3:1 pentane/

diethyl ether. The yellow eluate was evaporated to dryness in vacuo to obtain **7B** as a yellow solid (0.010 g, 0.024 mmol, 29%).

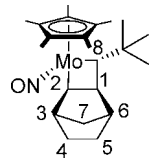


IR (Nujol): $\nu_{NO}$ 1596 cm$^{-1}$. $^1$H NMR ($C_6D_6$, 400 MHz, 25 °C, $\delta$): 6.07 (1H, dd ($^3J_{HH}$ = 7.1, 2.5), C2*H*), 3.50 (1H, d ($^3J_{HH}$ = 6.4), C8*H*), 2.29 (2H, d ($^2J_{HH}$ = 20.3), C7$H_2$), 1.78 (15H, s, Cp*$CH_3$), 1.43 (1H, m (overlapping), C4$H_2$ or C5$H_2$), 1.24 (9H, s, $^t$Bu$CH_3$), 1.09 (1H, m (overlapping), C4$H_2$ or C5$H_2$), 0.50 (1H, d ($^3J_{HH}$ = 10.0), C3*H*), −0.39 (1H, d ($^3J_{HH}$ = 10.0), C6*H*), −0.45 (1H, t ($^3J_{HH}$ = 6.4), C1*H*). $^{13}$C{$^1$H} NMR ($C_6D_6$, 100 MHz, 25 °C, $\delta$): 136.9 (C2 or C8), 132.8 (C2 or C8), 109.4 (Cp* quat C), 43.9 ($^t$Bu quat C), 43.0 (C3 or C6), 42.1 (C3 or C6), 34.3 (C4,5, or 7), 33.2 ($^t$BuCH$_3$), 32.0 (C4, C5, or C7), 28.6 (C4, C5, or C7), 25.4 (C1), 11.1 (Cp*CH$_3$). MS (EI, 100 °C): *m*/*z* 427 [M]$^+$.

**Complex 8F. 1** (0.050 g, 0.124 mmol) was dissolved in 1-hexene (0.555 g) and diluted with cyclohexane (5.7 g). The resulting pink solution darkened to a brown color over 18 h. The solution was then evaporated to dryness, and the residue was extracted with pentane (2 mL). The pentane extracts were loaded onto a column of neutral alumina (3 × 0.5 cm) prepared in pentane. The column was washed with pentane (10 mL). A yellow band was then eluted using 4:1 pentane/diethyl ether (8 mL) and collected. The yellow eluate was evaporated to obtain **8F** as a yellow solid (0.015 g, 0.036 mmol, 29%).

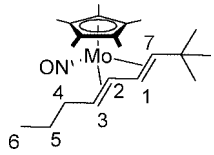


IR (Nujol): $\nu_{NO}$ 1600 cm$^{-1}$. $^1$H NMR ($C_6D_6$, 400 MHz, 25 °C, $\delta$): 3.36 (1H, ddd ($^3J_{HH}$ = 13.7, 10.7, 3.5), C3*H*), 3.18 (1H, dd ($^3J_{HH}$ = 12.6, 10.5), C1*H*), 2.11 (1H, d ($^3J_{HH}$ = 12.6), C7*H*), 1.97 (1H, m, C4$H_2$), 1.68 (15H, s, Cp*$CH_3$), 1.59−1.53 (4H, m (overlapping), C2*H*, C4$H_2$, and C5$H_2$), 1.24 (9H, s, $^t$Bu$CH_3$), 1.02 (3H, t ($^3J_{HH}$ = 7.2), C6$H_3$). $^{13}$C{$^1$H} NMR ($C_6D_6$, 100 MHz, 25 °C, $\delta$): 105.4 (Cp* quat), 99.6 (C7), 89.3 (C1 or C3), 88.7 (C1 or C3), 77.6 (C2), 35.6 (C4 or C5), 35.5 ($^t$Bu quat C), 33.6 ($^t$BuCH$_3$), 28.3 (C4 or C5), 14.3 (C6), 11.3 (Cp*CH$_3$). HRMS-EI *m*/*z*: [M]$^+$ calcd for $^{98}$MoC$_{21}$H$_{35}$NO 415.17727; found 415.17742.

**Complex 9F. 1** (0.059 g, 0.140 mmol) was dissolved in 1,7-octadiene (0.533 g) and diluted with cyclohexane (6.1 g). The resulting pink solution darkened to a brown color over 42 h. The solution was then evaporated to dryness, and the residue was extracted with pentane (2 mL). The pentane extracts were then loaded onto a column of neutral alumina (3 × 0.5 cm) prepared in pentane. The column was washed with pentane (10 mL). A yellow band was then eluted using 4:1 pentane/diethyl ether (8 mL) and collected. The yellow eluate was evaporated to dryness in vacuo to obtain **9F** as a yellow solid (0.020 g, 0.046 mmol, 33%).

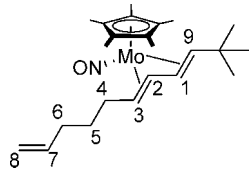


IR (Nujol): $\nu_{NO}$ 1600 cm$^{-1}$. $^1$H NMR ($C_6D_6$, 400 MHz, 25 °C, $\delta$): 5.83 (1H, ddt ($^3J_{HH}$ = 16.8, 10.2, 6.7), C7*H*), 5.08 (1H, ddd ($^3J_{HH}$ = 16.8, 3.3, 1.5), C8$H_2$), 5.03 (1H, d ($^3J_{HH}$= 10.2), C8$H_2$), 3.31 (1H, ddd ($^3J_{HH}$ = 13.1, 11.2, 3.9), C2*H*), 3.18 (1H, dd ($^3J_{HH}$ = 13.1, 10.2), C3*H*), 2.16 (2H, overlapping, C6$H_2$), 2.14 (2H, overlapping, C4$H_2$), 2.13 (1H, overlapping, C9*H*), 2.10 (2H, overlapping, C5$H_2$), 1.68 (15H, s, Cp*$CH_3$), 1.48 (1H, m, C1*H*), 1.24 (9H, s, $^t$Bu$CH_3$). $^{13}$C{$^1$H} NMR ($C_6D_6$, 100 MHz, 25 °C, $\delta$): 139.4 (C7), 115.2 (C8), 105.5 (Cp* quat), 99.6 (C9), 89.4 (C3), 88.6 (C1), 77.3 (C2), 35.5 ($^t$Bu quat), 34.4 (C4, C5, or C6), 34.0 (C4, C5, or C6), 33.6 ($^t$BuCH$_3$), 32.8 (C4, C5, or C6), 11.3 (Cp*CH$_3$). MS (EI, 100 °C): *m*/*z* 441 [M]$^+$.

**Complex 10F. 1** (0.060 g, 0.149 mmol) was dissolved in allylbenzene (1.0 g) and diluted with cyclohexane (5.8 g). The resulting pink solution darkened to a brown color over 18 h. The solution was then evaporated to remove solvent, and the residue was extracted with pentane (2 mL). The pentane extracts were loaded onto a column of neutral alumina (3 × 0.5 cm) prepared in pentane. The column was eluted with pentane (10 mL), and the colorless eluate was collected. The solvent was then removed in vacuo to obtain **11** (0.196 g, 0.829 mmol, 5.6 equiv) as a colorless liquid (see characterization data below). A yellow band was then eluted from the column using 4:1 pentane/diethyl ether (8 mL) and collected. The yellow eluate was then evaporated to dryness in vacuo, and the residue was recrystallized from pentane at −30 °C to obtain **10F** as yellow crystals (0.016 g, 0.036 mmol, 24%).

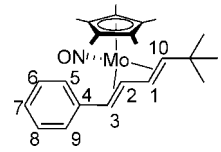


IR (Nujol): $\nu_{NO}$ 1603 cm$^{-1}$. $^1$H NMR ($C_6D_6$, 400 MHz, 25 °C, $\delta$): 6.95−7.27 (5H, m (overlapping), aryl C*H*), 4.46 (1H, d ($^3J_{HH}$ = 13.3), C3*H*), 3.43 (1H, dd ($^3J_{HH}$ = 12.0, 10.0), C1*H*), 2.43 (1H, dd ($^3J_{HH}$ = 13.3, 10.0), C2*H*), 2.25 (1H, d ($^3J_{HH}$ = 12.0), C10*H*), 1.46 (15H, s, Cp*$CH_3$), 1.24 (9H, s, $^t$Bu$CH_3$). $^{13}$C{$^1$H} NMR ($C_6D_6$, 100 MHz, 25 °C, $\delta$): 140.9 (aryl quat C), 128.9 (aryl C), 128.8 (aryl C), 128.7 (aryl C), 126.0 (aryl C), 106.1 (Cp* quat), 99.3 (C10), 89.3 (C1 or C3), 82.2 (C1 or C3), 76.6 (C2), 35.6 ($^t$Bu quat), 33.5 ($^t$BuCH$_3$), 10.6 (Cp*CH$_3$). HRMS-EI *m*/*z*: [M]$^+$ calcd for $^{98}$MoC$_{24}$H$_{33}$NO 449.16162; found 449.16166.

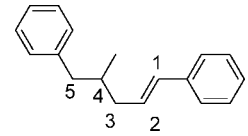


**(*E*)-(4-Methylpent-1-ene-1,5-diyl)dibenzene (11).** $^1$H NMR ($C_6D_6$, 400 MHz, 25 °C, $\delta$): 6.68−6.45 (10H, m overlapping, aryl C*H*), 5.72 (1H, d ($^3J_{HH}$ = 15.9), C1*H*), 5.50 (1H, dt ($^3J_{HH}$ = 15.9, 7.2), C2*H*), 1.98 (1H, dd ($^2J_{HH}$ = 13.3, $^3J_{HH}$ = 6.3), C5$H_2$), 1.70 (1H, dd ($^2J_{HH}$ = 13.3, $^3J_{HH}$ = 6.3), C5$H_2$), 1.55 (1H, dt ($^2J_{HH}$ = 14.0, $^3J_{HH}$ = 7.2), C3$H_2$), 1.33 (1H, dt ($^2J_{HH}$ = 14.0, $^3J_{HH}$ = 7.2), C3$H_2$), 1.18 (1H, ddd ($^3J_{HH}$ = 7.2, 6.8, 6.3), C4*H*), 0.25 (3H, d ($^3J_{HH}$ = 6.8), Me). $^{13}$C{$^1$H} NMR ($C_6D_6$, 100 MHz, 25 °C, $\delta$): 141.8 (aryl quat C), 138.6 (aryl quat C), 132.3 (C1), 129.9 (2 aryl C), 129.6 (C2), 129.1 (2 aryl C), 128.8 (2 aryl C), 127.5 (aryl para C), 126.8 (2 aryl C), 126.5 (aryl para C), 43.9 (C5), 40.75 (C3), 36.1 (C4), 19.9 (Me). MS (EI, 150 °C): *m*/*z* 236.1 [M]$^+$.

**X-ray Crystallography.** Data collection for each compound was carried out at −100 ± 1 °C on a Rigaku AFC7/ADSC CCD diffractometer or on a Bruker X8 APEX diffractometer, using graphite-monochromated Mo Kα radiation.

Data for **2B** were collected to a maximum 2$\theta$ value of 55.2° in 0.5° oscillations. The structure was solved by direct methods[22] and expanded using Fourier techniques. All non-hydrogen atoms were refined anisotropically, and all hydrogen atoms were included in

fixed positions. The final cycle of full-matrix least-squares analysis was based on 3600 observed reflections and 216 variable parameters.

Data for **2C** were collected to a maximum $2\theta$ value of 55.8° in 0.5° oscillations. The structure was solved by direct methods[22] and expanded using Fourier techniques. All non-hydrogen atoms were refined anisotropically; hydrogen atoms H01 (the hydride), H2, and H6 were refined isotropically, and all other hydrogen atoms were included in fixed positions. The final cycle of full-matrix least-squares analysis was based on 4608 observed reflections and 228 variable parameters.

Data for **3F** were collected to a maximum $2\theta$ value of 55.0° in 0.5° oscillations. The structure was solved by direct methods[22] and expanded using Fourier techniques. The coupled organic ligand and the nitrosyl ligand are disordered in two orientations. Restraints were used to maintain similar geometries for the related segments, namely, the *tert*-butyl groups, the cyclohexane rings, and the nitrosyl ligands. Overlapping atoms (N1 and C23, N2 and C2, C8 and C29, and C11 and C32) were refined isotropically; all other non-hydrogen atoms were refined anisotropically. Hydrogen atoms H2, H3, H23, and H24 were refined isotropically, and all other hydrogen atoms were included in fixed positions. The final cycle of full-matrix least-squares analysis was based on 4157 observed reflections and 322 variable parameters.

Data for **5D** were collected to a maximum $2\theta$ value of 49.8° in 0.5° oscillations. The structure was solved by direct methods[22] and expanded using Fourier techniques. All non-hydrogen atoms were refined anisotropically; hydrogen atoms H1, H2, and H9 were refined isotropically, and all other hydrogen atoms were included in fixed positions. The final cycle of full-matrix least-squares analysis was based on 3966 observed reflections and 255 variable parameters.

Data for **5F** were collected to a maximum $2\theta$ value of 53.1° in 0.5° oscillations. The structure was solved by direct methods[22] and expanded using Fourier techniques. The cyclooctenyl ring was disordered at C5, C6, and C7. The disorder was modeled with two orientations of 40% and 60% occupancy. Constraints were used to keep the related bond lengths in the disordered region equivalent. The three disordered carbons were refined isotropically; all other non-hydrogen atoms were refined anisotropically. Hydrogen atoms H2, H3, and H9 were refined isotropically, and all other hydrogen atoms were included in fixed positions. The final cycle of full-matrix least-squares analysis was based on 4201 observed reflections and 255 variable parameters.

Data for **6** were collected to a maximum $2\theta$ value of 55.1° in 0.5° oscillations. The structure was solved by direct methods[22] and expanded using Fourier techniques. All non-hydrogen atoms were refined anisotropically; hydrogen atoms H1, H2, and H9 were refined isotropically, and all other hydrogen atoms were included in fixed positions. The final cycle of full-matrix least-squares analysis was based on 5599 observed reflections and 309 variable parameters.

For each structure neutral-atom scattering factors were taken from Cromer and Waber.[23] Anomalous dispersion effects were included in $F_{calc}$;[24] the values for $\Delta f'$ and $\Delta f''$ were those of Creagh and McAuley.[25] The values for mass attenuation coefficients are those of Creagh and Hubbell.[26] All calculations were performed using the CrystalClear software package of Rigaku/MSC,[27] or Shelxl-97.[28] X-ray crystallographic data for the six structures are presented in Table 2 and in the cif files.

**Acknowledgment.** We are grateful to NSERC of Canada for support of this work in the form of grants to P.L.

**Supporting Information Available:** 2D NMR data (COSY and HMQC) for **2B** and CIF files providing full details of crystallographic analyses of complexes **2B**, **2C**, **3F**, **5D**, **5F**, and **6**. This material is available free of charge via the Internet at http://pubs.acs.org.

OM800157S

(22) SIR92: Altomare, A.; Cascarano, M.; Giacovazzo, C.; Guagliardi, A. *J. Appl. Crystallogr.* **1993**, *26*, 343.

(23) Cromer, D. T.; Waber, J. T. *International Tables for X-ray Crystallography*; Kynoch Press: Birmingham, 1974; Vol. IV.

(24) Ibers, J. A.; Hamilton, W. C. *Acta Crystallogr.* **1964**, *17*, 781–782.

(25) Creagh, D. C.; McAuley, W. J. *International Tables of X-ray Crystallography*; Kluwer Academic Publishers: Boston, 1992; Vol. C.

(26) Creagh, D. C.; Hubbell, J. H. *International Tables for X-ray Crystallography*; Kluwer Academic Publishers: Boston, 1992; Vol. C.

(27) *CrystalClear*: Version 1.3.5b20; Molecular Structure Corporation, 2002.

(28) Sheldrick, G. M. *SHELXL97*; University of Göttingen: Germany, 1997.